Multiscale model reduction of artificial ground freezing

Sergei Stepanov*, Maria Vasilyeva and Denis Spiridonov

II International Conference «Multiscale methods and Large-scale Scientific Computing»

August 15-17, 2018

Motivation

- Construction in northern and Arctic regions of Russia takes place in the difficult climate and engineering geological.
- Design construction in these regions require especially careful engineering researches and the organization of observations over natural processes around the planned construction.
- Permafrost in Yakutia is different from some other, because of extreme complexity of frozen soil distribution. Thereby, during engineering exploration of territory of Yakutia, it is necessary to develop measures to manage the interaction between permafrost and engineering constructions to ensure the effective exploitation of already constructed objects.

Mathematical Model

We conduct numerical research of problem of heat distribution in permafrost. The following mathematical model is used:

$$\left(\alpha(\phi) + \rho^{+} L \phi'\right) \frac{\partial T}{\partial t} - \operatorname{div}\left(\lambda(\phi) \operatorname{grad} T\right) = 0,$$

describing the heat transfer processes in the frozen and thawed soils. This model takes into account the presence of phase transitions of pore water in the soil at a given temperature phase transition T^* in domain $\Omega = \Omega^- \cup \Omega^+$:

$$\Omega^+(t) = \{\mathsf{x} | \mathsf{x} \in \Omega, T(\mathsf{x}, t) > T^*\},$$

$$\Omega^-(t) = \{\mathsf{x} | \mathsf{x} \in \Omega, T(\mathsf{x}, t) < T^*\}.$$

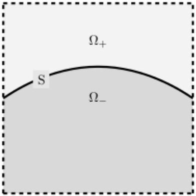

Mathematical Model

$$\phi_\Delta = \begin{cases} 0, & T \leqslant T^* - \Delta, \\ \dfrac{T - T^* + \Delta}{2\Delta}, & T^* - \Delta < T < T^* + \Delta, \\ 1, & T \geqslant T^* + \Delta, \end{cases}$$

$$\alpha(\phi) = \rho^- c^- + \phi(\rho^+ c^+ - \rho^- c^-), \qquad \lambda(\phi) = \lambda^- + \phi(\lambda^+ - \lambda^-),$$

$$c^- \rho^- = (1-m) c_{sc} \rho_{sc} + m c_i \rho_i, \qquad \lambda^- = (1-m)\lambda_{sc} + m\lambda_i,$$

$$c^+ \rho^+ = (1-m) c_{sc} \rho_{sc} + m c_w \rho_w, \qquad \lambda^+ = (1-m)\lambda_{sc} + m\lambda_w.$$

Initial and boundary conditions

Initial condition

$$T(\mathsf{x}, 0) = T_0, \quad \mathsf{x} \in \Omega,$$

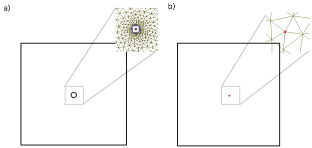

Figure: Boundary conditions on specific geometries

Boundary conditions

boundary conditions on circle boundary or in point:

$$[q \cdot n] = g + w(T - T_R), \quad \boldsymbol{x} \in \Gamma_b$$

- if $g = 0$ and $w = \frac{1}{\epsilon}$ then Dirichlet boundary condition,
- if $g \neq 0$ and $w = 0$ then Neumann boundary condition,
- if $g = 0$ and $w \neq 0$ then Robin boundary condition.

Fine scale approximation

The problem on a new time layer is formulated in the following variational form: find $T^{k+1} \in V$ such that

$$m(T^{k+1}, v) + a(T^{k+1}, v) = m(T^k, v) + [q \cdot n], \quad \forall v \in V,$$

where $T^k = T(t^k) \in V$ and k is the number of the time layer. Here V is a some suitable functional space.

$$m(T^{k+1}, v) = \frac{1}{\tau} \int_\Omega \left(\alpha(\phi_\Delta^k) + \rho^+ L \phi_\Delta'^k \right) T^{k+1} \, v \, dx,$$

$$a(T^{k+1}, v) = \int_\Omega \left(\lambda(\phi_\Delta^k) \operatorname{grad} T^{k+1}, \operatorname{grad} v \right) dx,$$

$$m(T^k, v) = \frac{1}{\tau} \int_\Omega \left(\alpha(\phi_\Delta^k) + \rho^+ L \phi_\Delta'^k \right) T^k \, v \, dx$$

and

$$[q \cdot n] = \int_{\Gamma_b} (g + w(T^{k+1} - T_R)) v ds,$$

GMsDGM

$$\omega_i = \bigcup \{K_j \in \mathcal{T}^H; \quad x_i \in \overline{K_j}\}.$$

Subdomains ω_i, K_j

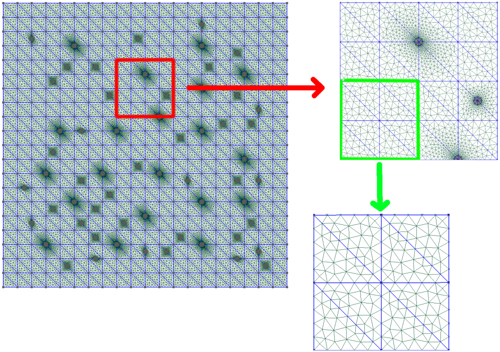

GMsDGM, "snapshots" space

In the "snapshots" space $(V_{snap}^{\omega_i})$, we consider the following:

$$
\begin{aligned}
-\operatorname{div}(k\nabla\psi_{l,j}^{snap}) &= 0, \ \ , x \in \ \omega_i, \\
\psi_{l,j}^{snap} &= \delta_l(x), \, x \in \ \partial\omega_i/\partial H, \\
\frac{\partial\psi_{l,j}^{snap}}{\partial n} &= 0, \, x \ \in \ \partial H,
\end{aligned}
$$

where $\delta_l(x)$ are some set of function defined on $\partial\omega_i$, e.g., unit source terms.

GMsDGM, offline space

To construct the offline space $V_{\text{off}}^{\omega_i}$, the following the local spectral problem is solved in the "snapshots" space:

$$A^{\text{off}}\Psi_l^{\text{off}} = \lambda_l^{\text{off}} S^{\text{off}} \Psi_l^{\text{off}},$$

where

$$A^{\text{off}} = [a_{mn}] = \int_{\omega_i} (k_m \nabla \psi_m^{snap}, \nabla \psi_n^{snap},) d\boldsymbol{x},$$

$$S^{\text{off}} = [s_{mn}] = \int_{\omega_i} (k_m \psi_m^{snap} \psi_n^{snap}) d\boldsymbol{x}.$$

GMsDGM, additional basis

For Dirichlet BC

$$
\begin{aligned}
&\int_{\omega_i} k \nabla T \nabla v d\boldsymbol{x} = 0, \\
&u = 0, \quad \boldsymbol{x} \in \partial\omega_i / \partial H, \\
&u = T_D, \quad \boldsymbol{x} \in \partial H.
\end{aligned}
$$

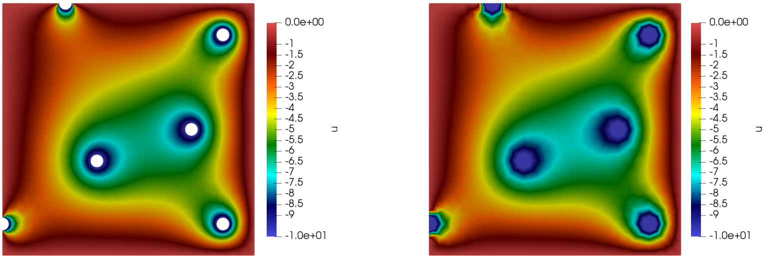

GMsDGM, additional basis

For Neumann BC

$$\int_{\omega_i} k \nabla T \nabla v d\boldsymbol{x} = \int_{\partial H} T_N v d\boldsymbol{s},$$
$$u = 0, \quad \boldsymbol{x} \in \partial \omega_i / \partial H.$$

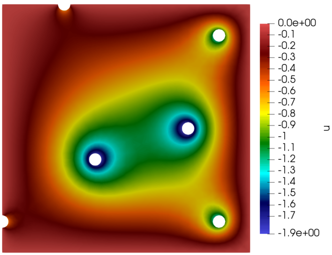

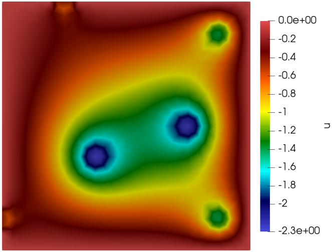

GMsDGM, additional basis

For Robin BC

$$\int_{\omega_i} k\nabla T \nabla v d\boldsymbol{x} + \int_{\partial H} \alpha T v d\boldsymbol{s} = \int_{\partial H} \alpha T_R v d\boldsymbol{s},$$
$$u = 0, \quad \boldsymbol{x} \in \partial\omega_i / \partial H.$$

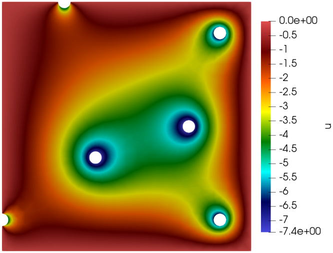

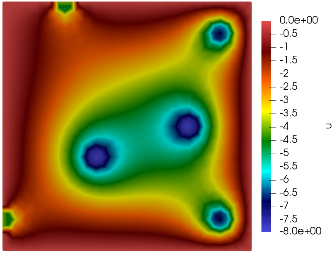

GMsDGM, Numerical experiments

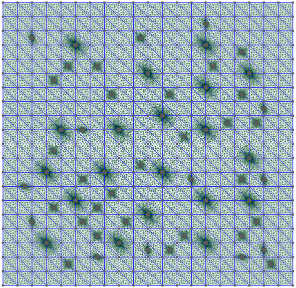

(a) with perforation (38824 vertices, 91179 elements)

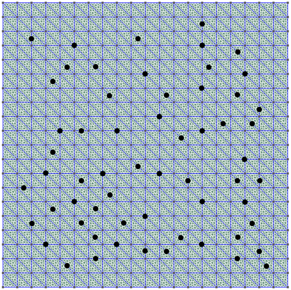

(b) without perforation (16999 vertices, 41437 elements)

GMsDGM, Numerical experiments

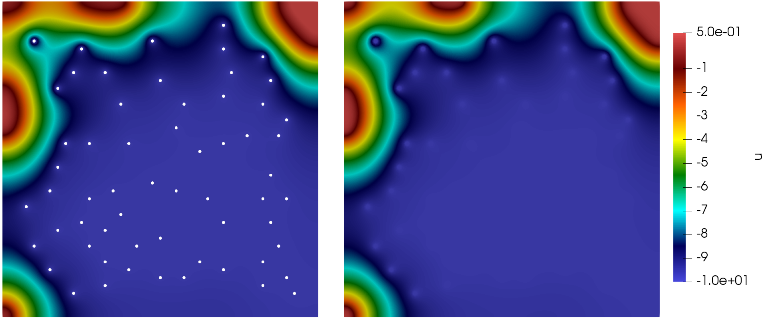

Figure: Numerical solution on a coarse grid 20×20 using 16 multiscale basis functions for Dirichlet boundary condition on 100 time of step. Left is case a) and right is case b).

GMsDGM, Numerical experiments

	DOF	$\|\|e\|\|_{L^2}$	$\|\|e\|\|_H$	DOF	$\|\|e\|\|_{L^2}$	$\|\|e\|\|_H$
		10×10			20×20	
$M = 1$	121	26.39	37.18	441	11.76	28.63
$M = 2$	2423	23.51	36.28	882	6.93	22.26
$M = 4$	484	12.53	24.24	1764	3.78	14.55
$M = 8$	968	6.93	16.96	3528	1.73	8.11
$M = 16$	1936	3.49	11.54	7056	0.71	4.53

Table: Solution errors for different number of multiscale basis functions and for different coarse grids on 10 time step. When we use Dirichlet boundary condition for case a).

GMsDGM, Numerical experiments

	DOF	$\|\|e\|\|_{L^2}$	$\|\|e\|\|_H$	DOF	$\|\|e\|\|_{L^2}$	$\|\|e\|\|_H$
		10×10			20×20	
$M = 1$	121	22.41	38.73	441	9.50	30.30
$M = 2$	242	20.46	36.55	882	6.79	26.14
$M = 4$	484	8.30	22.80	1764	3.08	15.54
$M = 8$	968	4.42	16.75	3528	1.23	9.99
$M = 16$	1936	2.43	13.31	7056	0.68	4.54

Table: Solution errors for different number of multiscale basis functions and different coarse grid on 10 time step. When we use Dirichlet boundary condition for case b).

GMsDGM, Numerical experiments

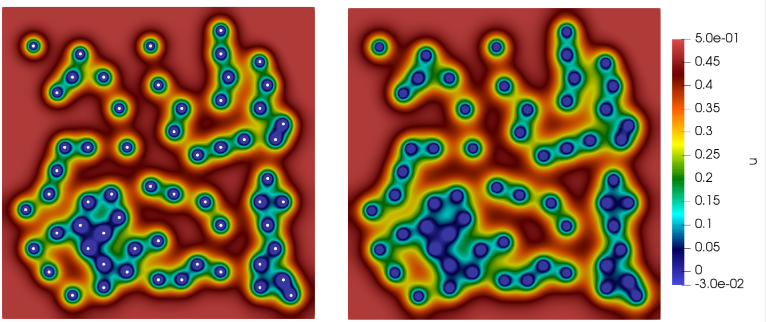

Figure: Numerical solution on a coarse grid 20×20 using 16 multiscale basis functions for Neumann boundary condition on 100 time of step. Left is case a) and right is case b).

GMsDGM, Numerical experiments

	DOF	$\|\|e\|\|_{L^2}$	$\|\|e\|\|_H$	DOF	$\|\|e\|\|_{L^2}$	$\|\|e\|\|_H$
		10×10			20×20	
$M = 1$	121	32.37	49.40	441	8.16	31.77
$M = 2$	242	24.65	41.15	882	3.96	21.13
$M = 4$	484	7.81	24.21	1764	3.11	17.27
$M = 8$	968	3.90	15.54	3528	0.92	7.63
$M = 16$	1936	1.54	9.74	7056	0.50	5.34

Table: Solution errors for different number of multiscale basis functions and different coarse grid on 10 time step. When we use Neumann boundary condition for case b).

GMsDGM, Numerical experiments

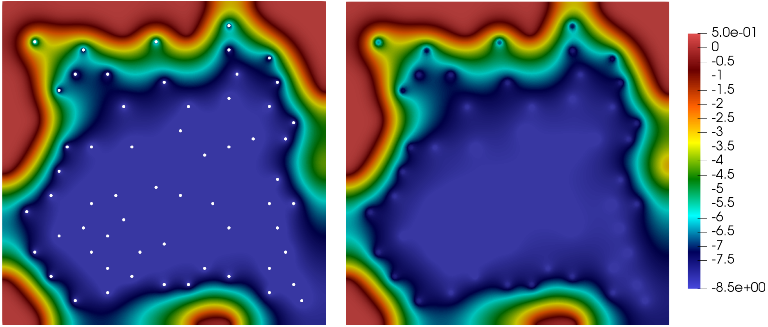

Figure: Numerical solution on a coarse grid 20×20 using 16 multiscale basis functions for Robin boundary condition on 100 time of step. Left is case a) and right is case b).

GMsDGM, Numerical experiments

	DOF	$\|\|e\|\|_{L^2}$	$\|\|e\|\|_H$	**DOF**	$\|\|e\|\|_{L^2}$	$\|\|e\|\|_H$
		10×10			20×20	
$M = 1$	121	31.76	40.61	441	16.43	25.95
$M = 2$	242	27.22	36.90	882	11.79	23.02
$M = 4$	484	10.12	17.42	1764	6.16	14.84
$M = 8$	968	6.05	12.63	3528	2.23	7.59
$M = 16$	1936	2.84	7.75	7056	0.82	3.99

Table: Solution errors for different number of multiscale basis functions and different coarse grid on 10 time step. When we use Robin boundary condition for case b).

GMsDGM, Numerical experiments

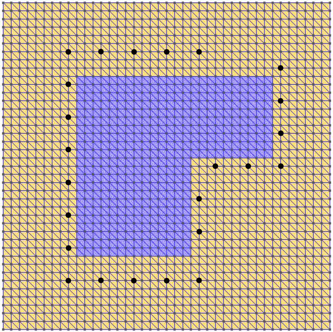

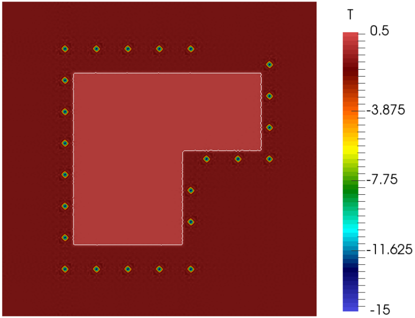

GMsDGM, Numerical experiments

	DOF	$\|\|e\|\|_{L^2}$	$\|\|e\|\|_H$	**DOF**	$\|\|e\|\|_{L^2}$	$\|\|e\|\|_H$
		10×10			20×20	
$M = 1$	121	20.11	45.82	441	7.22	28.64
$M = 2$	242	16.32	40.01	882	4.04	20.15
$M = 4$	484	7.43	25.01	1764	2.55	15.68
$M = 8$	968	4.02	17.14	3528	1.09	8.51
$M = 16$	1936	1.80	12.18	7056	0.47	4.90

Table: Solution errors for different number of multiscale basis functions and different coarse grid on 10 time step. When we use Dirichlet boundary condition.

GMsDGM, Numerical experiments

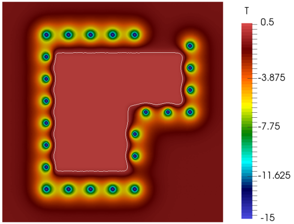

Figure: The temperature distribution for t = 10 days after beginning work seasonal-cooling devices (top to bottom). The solution on a coarse grid 20×20 using 16 multiscale basis functions.

GMsDGM, Numerical experiments

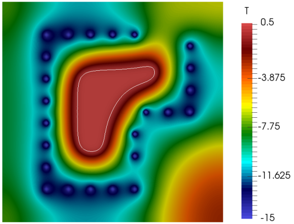

Figure: The temperature distribution for t = 150 days after beginning work seasonal-cooling devices (top to bottom). The solution on a coarse grid 20×20 using 16 multiscale basis functions.

Summary

In this paper, we study the different boundary condition for a solution of the heat transfer problem with phase change using Stefan model.
We construct reduced order model using Generalized Multiscale Finite Element Method.
Our results show that the presented method give good approximation of the solution and reduce size of system.

Thank you for your attention!